An Online Sleep Apnea Detection Method Based on Recurrence Quantification Analysis

Hoa Dinh Nguyen, Brek A. Wilkins, Qi Cheng, *Senior Member, IEEE*, and Bruce Allen Benjamin

***Abstract*—This paper introduces an online sleep apnea detection method based on heart rate complexity as measured by recurrence quantification analysis (RQA) statistics of heart rate variability (HRV) data. RQA statistics can capture nonlinear dynamics of a complex cardiorespiratory system during obstructive sleep apnea. In order to obtain a more robust measurement of the nonstationarity of the cardiorespiratory system, we use different fixed amount of neighbor thresholdings for recurrence plot calculation. We integrate a feature selection algorithm based on conditional mutual information to select the most informative RQA features for classification, and hence, to speed up the real-time classification process without degrading the performance of the system. Two types of binary classifiers, i.e., support vector machine and neural network, are used to differentiate apnea from normal sleep. A soft decision fusion rule is developed to combine the results of these classifiers in order to improve the classification performance of the whole system. Experimental results show that our proposed method achieves better classification results compared with the previous recurrence analysis-based approach. We also show that our method is flexible and a strong candidate for a real efficient sleep apnea detection system.**

***Index Terms*—Feature selection, recurrence quantification analysis (RQA), sleep apnea detection, soft decision fusion.**

I. Introduction

OBSTRUCTIVE sleep apnea (OSA) is a disorder in which a person experiences periodic disruption in breathing during sleep. An obstructive apneic episode is defined as the absence of airflow for at least 10 s, and may happen hundreds of times a night without individuals knowing they have OSA. This is a common problem with major health implications such as excessive daytime drowsiness, nonrestorative sleep, decreased memory, depression, and even serious cardiac arrhythmias. It has been linked to increased risks of high blood pressure, myocardial infarction, stroke, and increased mortality rates. Fortunately, sleep apnea is a treatable condition. However, most individuals with OSA are not identified and remain untreated [1].

Polysomnography (PSG) is a standard approach to recognize sleep apnea, which is based on the comprehensive monitoring of cardiorespiratory and sleep signals. PSG generally requires an overnight stay in a hospital for sufficient collection of signals related to OSA [2]. This can be an uncomfortable and inconvenient experience for individuals because it often disturbs or inhibits normal sleep and is often expensive.

Alternatively, the ECG signal is very promising for OSA detection since it offers a more convenient data collection procedure [3]–[6]. At present, new and low-priced 1-lead ECG recorders are already available, in which only two or three electrode attachments are needed [7]. ECG measurements provide an alternative view of physiological changes corresponding to sleep apnea behavior/severity. In 2000, the organizers of the Physionet database repository recognized the importance and potential use of the ECG signals in diagnosing sleep apnea. As a result, they hosted a challenge where various research teams introduced a number of different methodologies for sleep apnea detection using the ECG alone [8]–[15]. Since then, many methods using the ECG signal to diagnose OSA have been developed. For example, McNames and Fraser [13] introduce a sleep apnea detection method using heart rate (HR) and pulse energy of ECG signals. Khandoker *et al.* [5] use support vector machine (SVM) with 28 features extracted from heart rate variability (HRV) data and ECG-derived respiration data using wavelet decomposition to detect OSA. The performance comparison between SVM and other classifiers, i.e., K-nearest neighbors (KNN), probabilistic neural network (PNN), and linear discriminant (LD) using the same features is also presented in [6]. Mendez *et al.* [4] explore both temporal features and spectral features extracted from power spectral densities of recurrence rate (RR) intervals and QRS area series, and use a bivariate time-varying autoregressive model at each heart beat for OSA detection. KNN and neural networks (NNs) are used to classify apneic data from normal data on a 1-min basis. Bsoul *et al.* [16] implement a real-time sleep apnea and hypopnea syndrome detection system using 111 features in both time and spectral domains extracted from ECG data. Those features include 18 time-domain statistical features extracted directly from ECG signals, two features from ECG-derived respiration signals [17], and 91 features extracted from the frequency domain of ECG signals.

In this paper, we introduce a new framework for OSA detection, which capitalizes on nonlinear dynamical information within HRV signals extracted from the ECG. HRV is the variation of the time distance between consecutive heartbeats. HRV reflects the heart's ability to detect, quickly respond, and adapt to changing intrinsic and extrinsic stimuli. Since apneic episodes cause changes to heart regulation during sleep, using HRV data for sleep apnea detection is very promising [18], [19]. Moreover, recurrence plots (RPs) [20], [21] of HRV data are believed to be

Manuscript received January 16, 2013; revised September 4, 2013; accepted November 17, 2013. Date of publication November 27, 2013; date of current version June 30, 2014.

H. D. Nguyen is with the Posts and Telecommunications Institute of Technology, Hanoi, Vietnam, 10000 (e-mail: hoadn@okstate.edu).

Q. Cheng is with the School of Electrical and Computer Engineering, Oklahoma State University, Stillwater, OK 74078 USA (e-mail: qi.cheng@okstate.edu).

B. A. Wilkins and B. A. Benjamin are with the Center for Health Sciences, Oklahoma State University, Tulsa, OK 74107 USA (e-mail: brek.wilkins@okstate.edu; bruce.benjamin@okstate.edu).

Digital Object Identifier 10.1109/JBHI.2013.2292928

immune to the effects of the nonstationarity of nonlinear time series, and hence can be used as a good tool for OSA detection. RPs and subsequent recurrence quantification analysis (RQA) of HRV allow for the statistical characterization of complex HR regulations. The use of recurrence analysis on nocturnal HR for sleep apnea detection was first introduced by Maier and Dickhaus [3]. They pointed out that RP/RQA is inferior to spectral methods. By choosing a different RP thresholding method with different parameters (embedding dimensions $m = 6$, delay $\tau = 10$, and eight different fixed amount of nearest neighbors (FAN) values) from their approach, we attempt to better capture HR dynamics associated with OSA, thereby improving the classification of apnea versus normal. Data used in this study have been divided into 1-min sections and the corresponding label for each section is either apnea (1) or normal (0). As a result, we are limited to measuring minute by minute changes in nonlinear HR complexity using RQA, i.e., the window step is 1 min. A subsequent decision of apnea or normal is made each minute. A feature selection algorithm is integrated into the detection system design to improve the computational speed without degrading the classification performance of the whole system. To exploit the complementary information of different classifiers, two types of binary classifiers, i.e., SVM and NN, are used. A soft decision fusion rule is proposed to combine the outputs of these two classifiers for performance improvement. Experimental results show that our proposed decision rule is effective in improving the classification performance of the whole system.

II. Materials and Methods

A. Datasets

In this paper, we use the Physionet Apnea-ECG database [1]. A total of 35 subjects with OSA are used (classes a, b, c). The records were labeled and scored by an expert for sleep apnea/hypopnea events on a 1-minute basis. Each record contains a set of reference annotations, one for each minute of the recording that indicates the presence or absence of apnea during that minute. More details of the data can be found in [1].

ECG signals are sampled at 100 Hz with 12-bit resolution. HRV data are extracted from the digitized ECG signals. In the following section, we present a method to extract RQA features from HRV data.

B. RPs and RQA

Recurrence, which was first introduced by Poincare [22] in 1890, is a fundamental characteristic of dynamic systems. In 1987, Eckmann *et al.* [23] proposed the method of RPs to visualize the trends within time series from complex dynamic systems. In order to obtain RPs of a time series, $u(t)$, the data must be embedded in a phase space using Takens' time delay method [24]. Let a phase state be defined as follows:

$$\vec{x}_i = [u(i), u(i+\tau), \ldots, u(i+(m-1)\tau)] \tag{1}$$

where τ is the delay and m is the dimension of the embedding phase space. To set the appropriate values of m and τ, one must estimate the number of representative system variables expected to influence the system of interest, as well as the time required to achieve variable independence to avoid redundancy, respectively [25]. It is estimated that six cardiorespiratory variables have direct and immediate influence on HR dynamics at any given moment, i.e., cardiac output [26], blood pressure [27], respiratory rate [28], SpO2, cardiac repolarization (QT interval) [29], and central venous return [30]. Therefore, $m = 6$ is used in the study on the dynamics of HRV data. The delay τ must be chosen large enough to avoid constructing state vectors that are autocorrelated [31]. Empirically, we see that $\tau = 10$ is sufficient for analyzing HRV data.

An RP of a time series $u(t)$ is an $N \times N$ matrix, each element of which is calculated by the following equation:

$$R_{i,j} = \Theta(\epsilon_i - \|\vec{x}_i - \vec{x}_j\|), i, j = 1, 2, \ldots, N \tag{2}$$

where $\Theta(\cdot)$ is the unit step function, ϵ_i is the cutoff distance, and $\|\cdot\|$ is the Euclidean norm. This means that if a space vector $\vec{x}_j$ is within a range of ϵ_i from vector $\vec{x}_i$, then $R_{i,j} = 1$; otherwise, $R_{i,j} = 0$. The cutoff distance ϵ_i can either be a constant value or vary such that there is a constant number of neighboring states surrounding each point of a trajectory. The latter is also known as the FAN method [23]. It is often difficult to choose a proper value of threshold ϵ_i because if ϵ_i is too small, there will be too few recurrences resulting in small recurrence statistic values, whereas too large ϵ_i may lead to a saturation of recurrences and an increase in all recurrence statistics. FAN is more advantageous for use on HRV data since it does not require attractors to be of a similar volume for the comparison of state-space behaviors. Instead, a predefined percentage of recurrence points is set for all states [32].

RQA refers to quantitative measures that describe the structures of RPs. There are ten commonly used RQA measures in the literature. These measures include RR, determinism (DET), maximum diagonal line length (L), maximum vertical line length (V), entropy of the distribution of diagonal lines ($ENTR$) [33], laminarity (LAM), mean diagonal line (MDL), trapping time (TT) [21], recurrence time type 1 (T_1), and recurrence time type 2 (T_2) [34]. As discussed earlier, by choosing the FAN method for RP calculation, the cutoff threshold ϵ_i changes at every state such that there is a fixed number of recurrence points found for each $\vec{x}_i$ of the RP. This means an RR is fixed. As a result, only nine RQA measures are considered as features in this study and they are described as follows.

L is the length of the longest diagonal line, while V is the length of the longest vertical line of an RP. In all the following statistical calculations relating to diagonal lines, the main diagonal line is discarded.

DET is the percentage of recurrent points forming diagonal lines in a RP with minimal length $l_{\min}$

$$DET = \frac{\sum_{l=l_{\min}}^{L} lP(l)}{\sum_{i,j=1}^{N} R_{i,j}} \tag{3}$$

where $P(l)$ is the histogram of the diagonal lines of length $l, l = l_{\min}, \ldots, L$.

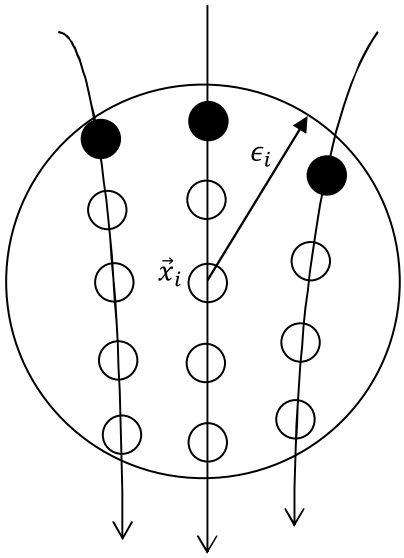

Fig. 1. Illustration of the recurrence points of the second type (solid dots) and the sojourn points (open dots) in $B_{\epsilon_i}(\vec{x}_i)$.

MDL is the average length of diagonal lines

$$MDL = \frac{\sum_{l=l_{\min}}^{L} lP(l)}{\sum_{l=l_{\min}}^{L} P(l)}. \tag{4}$$

$ENTR$ measures the Shannon entropy of the distribution of diagonal lines

$$ENTR = -\sum_{l=l_{min}}^{L} p(l)\ln p(l) \tag{5}$$

where $p(l)$ is the probability of the diagonal line having a length of l, $p(l) = \frac{P(l)}{\sum_{l=l_{\min}}^{L} P(l)}$.

LAM stands for the percentage of recurrence points forming vertical lines with minimum length of $v_{\min}$, which is so-called *laminarity*

$$LAM = \frac{\sum_{v=v_{\min}}^{V} vP(v)}{\sum_{i,j=1}^{N} R_{i,j}} \tag{6}$$

where $P(v)$ is the histogram of vertical lines of the length v, $v = v_{\min}, \ldots, V$.

TT represents the average length of vertical lines. It indicates how long the system remains in a specific state

$$TT = \frac{\sum_{v=v_{\min}}^{V} vP(v)}{\sum_{v=v_{\min}}^{V} P(v)}. \tag{7}$$

Consider a particular state $\vec{x}_i$. Let $B_{\epsilon_i}(\vec{x}_i) = \{\vec{x} : \|\vec{x} - \vec{x}_i\| \leq \epsilon_i\}$ denote a set of its recurrence points, which includes all dots in Fig. 1. These recurrence points form a sequence in the order of their appearances on a trajectory, i.e., $\{\vec{x}_{t_1}, \vec{x}_{t_2}, \ldots, \vec{x}_{t_{B_i}}\}$, where B_i is the cardinality of $B_{\epsilon_i}(\vec{x}_i)$. From this, the recurrence time of the first type T_1 is the average of all $t_{j+1} - t_j$, $j = 1, \ldots, B_i - 1$, $i = 1, \ldots, N$ and it measures the evolution of the constructed phase states.

The recurrence points of the second type are those points just getting inside $B_{\epsilon_i}(\vec{x}_i)$ from outside. They are denoted as the dark solid dots in Fig. 1. The trajectory may stay inside the neighborhood for a while, thus generating a sequence of points designated as open dots in Fig. 1. These are called *sojourn points* [34]. Recurrence time of the second type (T_2) is the average time difference between adjacent dark dots on a trajectory. It denotes the average time required for the system to return to a specific state after removing sojourn points.

These measures form a set of RQA statistics of each RP. Given time-series data, by using different values of FAN we obtain different sets of RQA statistics. In order to capture the nonstationarity of the human system by using RPs, we attempt to extract a more comprehensive profile representation of the dynamics by applying various fixed numbers of neighbors for RPs calculation. Eight different FAN values are used (2.5%, 5%, 7.5%, 10%, 12.5%, 15%, 17.5%, and 20%). Therefore, there are a total of 72 RQA features created for each HRV series.

C. Feature Selection

A set of 72 RQA features is large and may contain redundant and/or irrelevant features for apnea detection. Using a large number of features also increases the processing time of classifiers that limits the potential application of real-time detection. Feature selection is needed to trim irrelevant features, leaving the most compact feature set while maintaining the performance of the classification system. Exhaustive search is conceptually straightforward but computationally expensive. There have been various sequential search-based approaches including best individual features [35], sequential forward search, sequential forward floating search [36], etc. Mutual information (MI) has been explored in greedy forward feature selection methods [37]–[40]. The use of MI as a search criterion can be justified as follows. It has been shown in [41] and [42] that the classification error is lower bounded by $P_e \geq \frac{H(C) - I(C;\mathbf{S}) - 1}{\log_2(N_C - 1)}$, where C is the class label; N_C is the number of classes; $\mathbf{S}$ is the set of features being used for classification; $H(C)$ is the Shanon entropy of class variable; $I(C;\mathbf{S})$ is the MI between class variable and the set of selected features. It is generally difficult to quantify directly the performance improvement of a classifier when selecting features. Therefore, MI is evaluated since increasing the MI can reduce the lower bound of the classification error for given $H(C)$.

Battiti [37] proposes an incremental search method, i.e., mutual information-based feature selection (MIFS). This method selects feature f into the existing feature subset $\mathbf{S}$ if $I(C;f) - \beta \sum_{s \in \mathbf{S}} I(f;s)$ is the largest. That is, feature f should be selected if it maximizes the MI with the class C and has minimum MI with every existing feature s in $\mathbf{S}$. The main disadvantage of this MIFS method is the difficulty in setting the parameter β. Especially, when the size of $\mathbf{S}$ becomes large, the selection algorithm tends to select features that are less correlated with the selected features while neglecting its correlation with the class label. In [39], β is set to be $1/|\mathbf{S}|$, where $|\mathbf{S}|$ is the cardinality of the selected feature subset and this can partly solve the problem aforementioned. However, the wide range of MI values may still

cause the bias [40]. To handle this issue, the normalized MI is introduced in [40].

The limitations of existing MIFS methods are twofolds. First, ideally, the feature with maximum conditional MI $I(C; f|\mathbf{S})$ should be selected. Existing methods approximate it by an alternative problem that maximizes $I(C; f)$ and minimizes $\sum_{s\in\mathbf{S}} I(f; s)$ through a weighted sum. This approximation helps facilitate the MI estimation since we do not have to deal with high-dimensional data. However, the conditional MI between f and C given the knowledge of $\mathbf{S}$ cannot be correctly represented by a function of the MI between f and C and the MI between f and every feature in $\mathbf{S}$. In other words, the feature that both maximizes $I(C; f)$ and minimizes $\sum_{s\in\mathbf{S}} I(f; s)$ is not necessary the one that maximizes $I(C; f|\mathbf{S})$. Second, current methods can select relevant features for classification but cannot eliminate redundant features if already selected. There is no step to reevaluate the redundancy of selected features when new features are added into the subset. As a result, the selected feature subset may not be the most compact one. We intend to find the most compact feature subset while maintaining the classification performance. The proposed feature selection method is described as follows.

- **Algorithm**:
  - Step 1: Set $\mathbf{F} \leftarrow$ "set of all D features"; $\mathbf{S} \leftarrow$ "empty set".
  - Step 2: Repeat until $\mathbf{F} = \emptyset$.
    1) Randomly select one feature $f_i \in \mathbf{F}$, compute conditional mutual information $I(C; f_i|\mathbf{S})$; set $\mathbf{F} \leftarrow \mathbf{F} \setminus \{f_i\}$.
    2) Feature selection: if $I(C; f_i|\mathbf{S}) > \gamma$; set $\mathbf{S} \leftarrow \mathbf{S} \cup \{f_i\}$.
    3) Validating $\mathbf{S}$:
       - if $|\mathbf{S}| = 1$ then goto (1).
       - else
         a) set $k = 1$.
         b) repeat until $k > |\mathbf{S}|$
            i) Compute $I(C; f_k|\mathbf{S} \setminus \{f_k\})$.
            ii) Set $k = k + 1$.
            iii) If $I(C; f_k|\mathbf{S} \setminus \{f_k\}) \leq \gamma$, then set $\mathbf{S} \leftarrow \mathbf{S} \setminus \{f_k\}$; set $k = 1$.
  - Step 3: Output selected feature subset $\mathbf{S}$.

In essence, this feature selection method aims at selecting any features that are relevant to the class label, but not redundant. The threshold γ is set at a reasonably small value such that it helps remove features containing pure noise. In this feature subset selection method, we integrate a redundancy evaluation step right after a new feature is selected into the subset. This step helps remove all redundant features emerging during the selection process. The evaluation step is similar to the idea of backward feature elimination. However, we only need to apply it to a small set of selected features instead of the whole original feature set, which helps reduce the computational effort significantly.

To calculate the required MI in the algorithm, the joint probability density functions (pdfs) of selected features are needed. These pdfs can be estimated using the Parzen window method [43]. Let vector $\mathbf{z}$ denote the values of selected features. Given m_c samples of $\mathbf{z}$ belonging to class c, the approximated conditional pdf $\hat{p}(\mathbf{z}|c)$ using the Parzen window method is

$$\hat{p}(\mathbf{z}|c) = \frac{1}{m_c} \sum_{i\in I_c} \phi(\mathbf{z} - \mathbf{z}_i, h) \tag{8}$$

where $c = 1, \ldots, N_C$; I_c is the set of indices of training samples $\mathbf{z}_i$ belonging to class c; $\phi(\cdot)$ is the window function; h is the window parameter. The estimation of pdf $\hat{p}(\mathbf{z}|c)$ can converge to the true one if $\phi(\cdot)$ and h are properly chosen [43]. In the literature, a Gaussian window is usually used

$$\phi(\tilde{\mathbf{z}}, h) = \frac{1}{(2\pi)^{D/2} h^D |\Sigma|^{1/2}} \exp\left(-\frac{\tilde{\mathbf{z}}'\Sigma^{-1}\tilde{\mathbf{z}}}{2h^2}\right) \tag{9}$$

where $\tilde{\mathbf{z}} = \mathbf{z} - \mathbf{z}_i$; D is the dimensions of sample $\tilde{\mathbf{z}}$; Σ is the covariance matrix of $\tilde{\mathbf{z}}$. In order to simplify the pdf estimation for high-dimensional data, "kernel independence" is assumed [44]. The general pdf estimate of a D-dimensional variable is then expressed as follows:

$$\hat{p}(\mathbf{z}|c) = \frac{1}{m_c} \sum_{i\in I_c} \prod_{d=1}^{D} \phi(z^{(d)} - z_i^{(d)}, h_d). \tag{10}$$

h_d in each dimension can be chosen as $h_d = 1.06\sigma_d m_c^{-1/5}$, where σ_d is the standard deviation of training data in dimension d [44].

The conditional MI $I(C; f_i|\mathbf{S})$ can be expressed in terms of conditional entropies as follows:

$$I(C; f_i|\mathbf{S}) = H(C|\mathbf{S}) - H(C|\mathbf{S}, f_i) \tag{11}$$

where $H(C|\mathbf{S})$ is the conditional entropy of class variable C given the selected features $\mathbf{S}$. The conditional entropy can be approximated as

$$\hat{H}(C|\mathbf{S}) = -\sum_{j=1}^{M}\sum_{c=1}^{N_C} p(c)\hat{p}(\mathbf{s}_j|c) \log \frac{\hat{p}(\mathbf{s}_j|c)p(c)}{\sum_{k=1}^{N_C} \hat{p}(\mathbf{s}_j|k)p(k)} \tag{12}$$

where $\mathbf{s}_j$ is the jth training sample, M is the total number of training samples, $p(c)$ is the prior probability of class c, which can be assumed as uniformly distributed indicating the least prior knowledge.

D. Classification

1) Binary "Soft" Decision Fusion: Different classifiers may have different decision making perspectives, and misclassified samples may not overlap in different classifiers. Therefore, combining the results from different classifiers may help compensate the information loss of respective classifiers, and could further increase the classification accuracy. As a result, classifier combination is a powerful tool for classification improvement in many fields of study [45]. In general, any classifier combination approach may belong to one of three categories: abstract level, rank level, and measurement level [46]. Majority voting [47]

is an abstract-level combination example. Examples of rank-level methods include weighted majority voting [48] and Borda count [45]. In the measurement level, the outputs of a classifier are scores reflecting the degrees of a sample belonging to individual classes, instead of the class labels. These scores are combined for final decision making. The combination methods of this level include sum-rule, product-rule, and max-rule [45].

Xie and Minn [49] investigate the application of four binary classifier combination methods for sleep apnea detection, such as max probability, average probability, product of probability (which all belong to the measurement level), and majority voting (abstract level). They show that classifier combination can help improve the classification performance.

The limitation of current decision fusion methodologies is that they do not take into account the quality of each classifier. Some classifiers may provide higher sensitivity, and others may have higher specificity, and vice versa. If the classifier quality information can be integrated in the decision fusion process, the global decision is believed to be more reliable. In this section, a binary soft decision fusion rule based on the confidence score maximization strategy is proposed. The new decision fusion rule belongs to the measurement level.

Outputs of binary classifiers are scores representing the probability that the sample belongs to either class. We denote the outputs of all K classifiers to be $\{T_k \in [0,1]\}, k = 1, \ldots, K$. These scores are fused together to provide a reliable final decision on the class of the data. We introduce the term "confidence score" for each class. This is a combination between the score T_k of classifier k and its classification quality. The confidence score of classifier k for each class can be formulated as follows:

Confidence score of class 1 (apnea)

$$\begin{aligned} Q_1^k &= T_k P^k(D^k = 1, H = 1) \\ &= T_k P^k(D^k = 1 | H = 1) P(H = 1). \end{aligned} \tag{13}$$

Confidence score of class 0 (normal)

$$Q_0^k = (1 - T_k) P^k(D^k = 0 | H = 0) P(H = 0) \tag{14}$$

where $P(H = 1)$ and $P(H = 0)$ are the prior probabilities of hypotheses apnea and normal, respectively; $P^k(D^k = 1|H = 1)$ and $P^k(D^k = 0|H = 0)$ are probabilities of correct decisions of classifier k for the two classes, which can be obtained from the training process.

These confidence scores represent soft decisions of all binary classifiers. It is shown by Kittler *et al.* [50] that the sum-rule is less sensitive to noise than other combination rules. Therefore, we combine confidence scores from all classifiers using the sum-rule, i.e., $Q_i = \sum_{k=1}^{K} Q_i^k, i \in \{0, 1\}$. The final decision is made by choosing the class with a highest confidence score $D = \arg\max_i Q_i$.

Indeed, this soft decision fusion rule is a weighted sum of the output scores of all binary classifiers. The weights being used are the qualities of individual classifiers combined with the prior knowledge of each class of the data. By changing the prior probabilities of the classes, the final decision will be affected. For example, with patients having a high chance of sleep apnea symptoms, the prior probability of apeic events during sleep can be set higher than that of normal people. This shows the flexibility of the proposed method. In this study, uniformly distributed probabilities are used since there are both apnea and normal data contained in each OSA record.

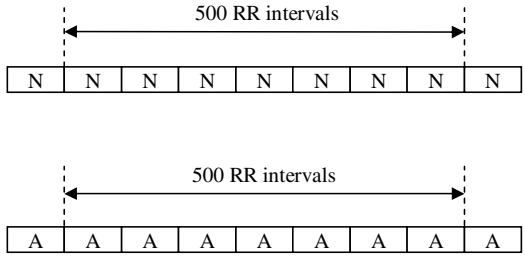

Fig. 2. Training data of binary classifiers. Each block is 1 min of HRV data. RPs are calculated based on a 500 RR interval window. Training data for class normal contain pure normal (*N*) blocks; training data for class apnea include pure apnea (*A*) blocks.

2) Binary Classifiers: Two most widely used binary classifiers, SVM and NN are adopted for classifier fusion.[1] SVM with kernel constructs a hyperplane with maximal margins to separate data into two classes in a higher dimensional feature space. Gaussian radial basis functions (RBF) are commonly used as kernels because the corresponding feature space is of infinite dimensions. SVM in [51] is followed except that the parameter γ of RBF is set to 0.001, and the cost C is set to 4 in order to keep the validation error rate under 1%. A ten neuron hidden-layer NN provided by the Matlab toolbox [52] is used. To assess the performance of classifiers, we use three metrics: sensitivity, specificity, and accuracy [49]. Specificity represents the ability to correctly classify normal data, while sensitivity reflects the ability to detect apneic events.

3) Classifier Training: Binary classifiers are trained using apneic and normal data separately. Fig. 2 illustrates training data of each class. RPs are calculated from two separate normal and apnea subsets, and RQA statistics of normal and apneic data are extracted, respectively. The window width for calculating RPs is set at 500 RR intervals, and the moving window step is set at five RR intervals. There are roughly a total of 62,000 RQA samples of the normal class and 59,000 RQA samples of the apneic events available. Each binary classifier is trained using one-third of the data (training set), and validated using the remaining two-thirds of it (validating set). Specifically, the data for training are selected in every three samples from the data pool resulting in the window step of 15 RR intervals. Empirically, given the rapid adaptability of the body system, we observe that significant dynamic changes will occur from window to window with this step. Therefore, the effect of overtraining is minimized. Threefold cross validation is adopted. The average classification performances are summarized in Table I and the classifier with the best classification performance is selected for testing.

[1]The proposed fusion framework is sufficiently general to integrate different number and/or types of binary classifiers.

TABLE I
CLASSIFICATION PERFORMANCE OF BINARY CLASSIFIERS AFTER TRAINING USING EITHER FULL FEATURE SET OR SELECTED FEATURE SUBSET

Classifier	All features				33 features			
	Sensitivity	Specificity	Accuracy	Processing time (10,000 samples)	Sensitivity	Specificity	Accuracy	Processing time (10,000 samples)
Neural Network	93.9 (%)	94.33 (%)	94.21 (%)	0.747 (s)	93.11 (%)	91.75 (%)	92.14 (%)	0.0524 (s)
SVM	99.34 (%)	99.25 (%)	99.28 (%)	80 (s)	98.93 (%)	98.68 (%)	98.75 (%)	29 (s)

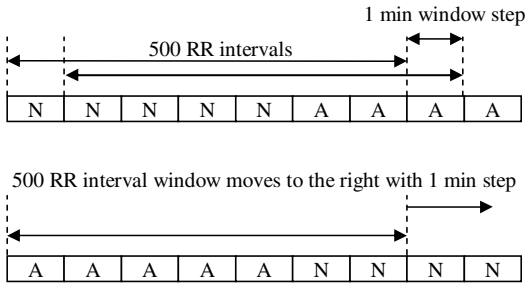

Fig. 3. Real data with a mixture of normal and apneic blocks. The ground truth of each window is determined by the content of newly added block on the right.

TABLE II
SELECTED RQA FEATURES

RQA statistics	FAN							
	2.5%	5%	7.5%	10%	12.5%	15%	17.5%	20%
DET	1	1	1	1	1	1	1	1
MDL	1	1	1	1	-	-	-	-
$ENTR$	-	-	-	-	-	-	-	-
L	-	-	-	-	-	-	-	-
LAM	1	1	1	1	1	1	1	1
TT	1	1	1	1	1	-	-	-
V	-	-	-	-	-	-	-	-
T_1	-	-	-	-	1	1	1	1
T_2	-	-	-	-	1	1	1	1

III. RESULTS AND DISCUSSIONS

A. Binary Classifier Performance

Table I presents all sensitivity, specificity, and accuracy rates of both NN and SVM after training. Training performances are obtained from datasets containing pure normal and apneic data. The results show that the normal and apnea classes can be well distinguished when pure data are considered.

The performance of these classifiers are expected to deteriorate when we apply to real data, which may contain the mixture of normal and apneic events within the window (see Fig. 3). Specifically, RPs are calculated based on a moving window of 500 RR intervals in real data with a 1-min-window step. There are many time points at which the observation window contains both normal and apneic data. The system makes decisions for the newly coming minute of data as a normal or apneic event based on the information of the whole window. With the mixture of normal and apneic data, the output scores of binary classifiers tend to become less extreme values. As a result, the classification accuracy of individual classifiers can be affected. In fact, the change in output scores of classifiers can be further used as an indicator of the boundaries between normal and apneic events, which will not be discussed in this paper.

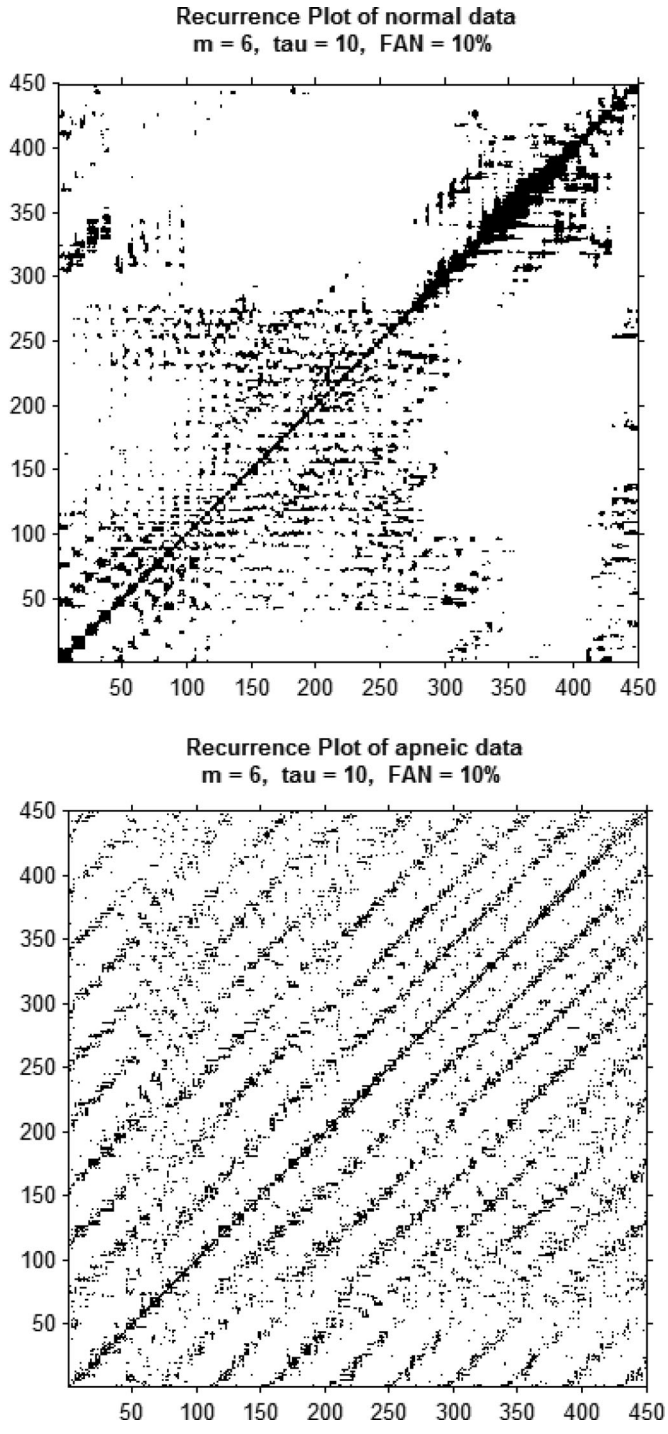

Fig. 4. Sample RPs of normal and apnea sleep. Data are extracted from record a01. RPs are calculated based on a window width of 500 RR intervals. In each of those figures, $R_{1,1}$ is located at the bottom left conner.

TABLE III
CLASSIFICATION PERFORMANCE OF THE SYSTEM ON REAL DATA

Classifier	All features			33 features		
	sensitivity	specificity	accuracy	sensitivity	specificity	accuracy
NN	85.57 (%)	79.09 (%)	83.23 (%)	85.46 (%)	78.96 (%)	82.92 (%)
SVM	93.72 (%)	65.88 (%)	84.14 (%)	90.11 (%)	76.34 (%)	83.41 (%)
Decision fusion	86.37 (%)	83.47 (%)	**85.26** (%)	85.81 (%)	81.69 (%)	**84.19** (%)

TABLE IV
COMPARISON BETWEEN DIFFERENT METHODS

Methods	Sensitivity (%)	Specificity (%)	Accuracy (%)
Soft decision fusion from SVM and NN using RQA statictics of HRV data	86.37	83.47	85.26
Bagging.REPTree using ECG data [49]	69.82	80.29	77.74
Best classification using RQA features [3]	66.8	73.8	76.7
Best classification using spectral features [3]	76.6	78.2	84.3
KNN applied on temporal and spectral features [4]	85	90	88
NN applied on temporal and spectral features [4]	89	86	88
SVM using RBF applied on wavelet features [5]	93.85	83.33	89
LD applied on wavelet features [6]	90	100	93
KNN applied on wavelet features [6]	80	90	83
PNN applied on wavelet features [6]	80	50	70

B. Feature Selection

The proposed feature selection method is applied to select the most compact feature subset from the 72 available RQA features. The final feature subset consists of 33 features as listed in Table II. In the Table, "1" represents a selected RQA feature in accordance with a specific value of FAN. Those selected features include all eight DET, all eight LAM, together with four MDL, five TT, four T_1, and four T_2 features.

Apneic events, which normally last from 20 s to over 1 min, usually occur *periodically* and *consecutively* in a span of more than 5 min. As a result, the cardiorespiratory dynamic change occurs periodically during sleep apnea. This leads to the appearance of diagonal and vertical patterns in the RPs of apneic events (see Fig. 4). Therefore, DET and LAM turn out to be the most useful features to distinguish the two sleeping conditions. Meanwhile, RQA features such as L, V, and $ENTR0$ do not appear to be closely related to cardiorespiratory changes as manifested by the structures of RPs between the two sleeping states.

The performance comparison between the classifiers using the selected feature subset and using the whole feature set is presented in Table I. The compact feature subset has minor effect on the accuracy of the classification system. Specifically, the accuracy of NN is reduced by 2.07%, while that of SVM is reduced by 0.52% if we use the selected feature subset. However, the processing time of both classifiers is significantly reduced. The processing time of NN is reduced by more than ten times, while that of SVM is improved by almost three times. This is especially important for real-time detection implementation.

The comparison between the two feature sets using the real data is summarized in Table III. There is a slight impact on all measures, i.e., sensitivity, specificity, and accuracy, when we switch from the full feature set to the compact feature subset. However, the accuracy rates of the system in the two cases are not much different. Specifically, the decrease of both sensitivity and specificity of NN are less than 0.1%, while the decrease of accuracy of NN is 0.31%. Meanwhile, the reduction of the accuracy of SVM is 0.73%. If we use the proposed soft decision fusion, the reduction of the accuracy of the whole system is only 1.07%.

C. Decision Fusion and Classification Efficiency

Table III tabulates the classification results of SVM and NN when they work separately, as well as when they are combined using the soft decision fusion rule. According to the results, soft decision fusion can help improve the classification *accuracy*. This is mainly because when there is a mixture of data between normal and apneic episodes, the output scores of individual classifiers become less extreme values. Additionally, there may be some nonoverlap misclassified samples among different classifiers. If these output scores are combined together, the information of individual classifiers may complement each other. Furthermore, the quality information of each classifier is used as the weight to combine its score with the other. As a result, the global decision becomes more reliable.

D. Comparison With Other Methods

In this section, we compare our work with some other recent methods based on ECG data to detect sleep apnea. Table IV presents a summary of classification performances of various methods obtained from [3]–[6], [49].

The experimental results show that our proposed OSA detection method based on only ECG data using soft decision fusion has good accuracy compared with other approaches. Specifically, our method outperforms the previous approach that introduced the use of RQA features for sleep apnea detection [3]. The main reason is that our method, with a different choice of RP parameters, effectively exploits the difference in nonlinear and

nonstationary dynamical information of HRV data during normal and apneic breathing. Empirically, we find that the complex cardiorespiratory system control changes acutely during night time obstructive sleep. RQA statistics of HRV data obtained from different FAN values can successfully capture this information for classification. Additionally, our soft decision fusion rule efficiently combines the outputs of different binary classifiers based on their performance qualities, and hence, helps improve decision accuracy on the real data.

It is noted that LD using wavelet features in [6] and NN with temporal and spectral features in [4] outperform our proposed method on this dataset. However, their performance is very sensitive to the type of classifiers and parameters selected. This implies that they may not generalize well to different datasets with different conditions. Our method, on the other hand, has fewer parameters that need to be tuned in training. We mainly capture HR dynamic features associated with OSA using different FAN values. Besides, classifier fusion is integrated in the framework to exploit the complementary information of different classifiers. Therefore, our approach is expected to be more robust and generalize well for different conditions.

The price to pay for the improve robustness, however, is increased computational time. With eight different FAN values, eight RPs have to be generated and a total of 72 features need to be calculated for each HRV window. Two different classifiers need to be trained separately. To reduce the computational time, feature selection is integrated in the framework, thus only 33 features needs to be calculated for each window.

IV. Conclusion

In this paper, we have proposed a new sleep apnea detection approach based on RQA statistics of HRV data, which are extracted from ECG signals. The RQA features extracted from HRV data using different FAN values help provide a detailed picture of the dynamical control of the cardiorespiratory system during normal and apneic sleeping. The use of only ECG data for sleep apnea detection is preferable to PSG data or the combination of ECG data and PSG data since it offers a more convenient data collection procedure. In addition, the new method includes an efficient soft decision fusion rule combining output scores of multiple binary classifiers and help improve the sleep apnea detection accuracy. Our experimental results in Section III illustrate the advantages of the proposed method in terms of higher classification accuracy compared with the previous approach based on recurrence analysis. There are still many possible ways to improve the classification performance in the real implementation of our method such as the change in the types and number of binary classifiers. Furthermore, a new feature selection algorithm integrated in our method is shown to be very efficient to select the most discriminative RQA features for classification. It helps reduce the computational time significantly during real-time detection, while maintaining acceptable classification performance. The mixture of apneic and normal events in the real data may lead to inconsistent output scores of binary classifiers and make them become less extreme values. These changes in outputs of classifiers may be exploited as an indicator of the boundaries between normal and apneic events. This will be investigated in our future work.

References

[1] A. L. Goldberger, L. A. N. Amaral, L. Glass, J. M. Hausdorff, P. Ch. Ivanov, R. G. Mark, J. E. Mietus, G. B. Moody, C.-K. Peng, and H. E. Stanley, "Physiobank, physiotoolkit, and physionet: Components of a new research resource for complex physiologic signals," *Circulation*, vol. 101, no. 23, pp. e215–e220, 2000.

[2] R. K. Kakkar and R. B. Berry, "Positive airway pressure treatment for obstructive sleep apnea," *Chest*, vol. 132, no. 3, pp. 1057–1072, 2007.

[3] C. Maier and H. Dickhaus, "Recurrence analysis of nocturnal heart rate in sleep apnea patients," *Biomed. Tech.*, vol. 51, no. 4, pp. 224–228, 2006.

[4] M. O. Mendez, A. M. Bianchi, M. Matteucci, S. Cerutti, and T. Penzel, "Sleep apnea screening by autoregressive models from a single ECG lead," *IEEE Trans. Inf. Technol. Biomed.*, vol. 56, no. 12, pp. 2838–2850, Dec. 2009.

[5] A. H. Khandoker, M. Palaniswami, and C. K. Karmakar, "Support vector machines for automated recognition of obstructive sleep apnea syndrome from ECG recordings," *IEEE Trans. Inf. Technol. Biomed.*, vol. 13, no. 1, pp. 37–48, Jan. 2009.

[6] A. H. Khandoker, C. K. Karmakar, and M. Palaniswami, "Automated recognition of patients with obstructive sleep apnoea using wavelet-based features of electrocardiogram recordings," *Comput. Biol. Med.*, vol. 39, pp. 88–96, 2009.

[7] J. W. Grier. (2008). "How to use 1-lead ECG recorders to obtain 12-lead resting ECGs and exercise ('stress') ECGs," [Online]. Available: http://www.ndsu.edu/pubweb/∼grier/1to12-lead-ECG-EKG.html

[8] M. J. Drinnan, J. Allen, P. Langley, and A. Murray, "Detection of sleep apnoea from frequency analysis of heart-rate variability," *Comput. Cardiol.*, vol. 27, pp. 259–262, 2000.

[9] M. Schrader, C. Zywietz, V. von Einem, B. Widiger, and G. Joseph, "Detection of sleep apnea in single channel ECGs from the PhysioNet data base," *Comput. Cardiol.*, vol. 27, pp. 263–256, 2000.

[10] P. K. Stein and P. P. Domitrovich, "Detecting OSAHS from patterns seen on heart-rate tachograms," *Comput. Cardiol.*, vol. 27, pp. 271–274, 2000.

[11] M. Ballora, B. Pennycook, P. Ch. Ivanov, A. Goldberger, and L. Glass, "Detection of obstructive sleep apnea through auditory display of heart-rate variability," *Comput. Cardiol.*, vol. 27, pp. 739–740, 2000.

[12] P. de Chazal, C. Heneghan, E. Sheridan, R. Reilly, P. Nolan, and M. O'Malley, "Automatic classification of sleep apnea epochs using the electrocardiogram," *Comput. Cardiol.*, vol. 27, pp. 745–748, 2000.

[13] J. McNames and A. Fraser, "Obstructive sleep apnea classification based on spectrogram patterns in the electrocardiogram," *Comput. Cardiol.*, vol. 27, pp. 749–752, 2000.

[14] J. E. Mietus, C.-K. Peng, P. Ch. Ivanov, and A. L. Goldberger, "Detection of obstructive sleep apnea from cardiac interbeat interval time series," *Comput. Cardiol.*, vol. 27, pp. 753–756, 2000.

[15] Z. Shinar, A. Baharav, and S. Akselrod, "Obstructive sleep apnea detection based on electrocardiogram analysis," *Comput. Cardiol.*, vol. 27, pp. 255–258, 2000.

[16] M. Bsoul, M. Minn, and L. Tamil, "Apnea MedAssist: Real-time sleep apnea monitor using single-lead ECG," *IEEE Trans. Inf. Technol. Biomed.*, vol. 15, no. 3, pp. 416–427, May 2011.

[17] G. B. Moody, R. G. Mark, A. Zoccola, and S. Matero, "Derivation of respiratory signals from multilead ECGs," *Comput. Cardiol.*, vol. 12, pp. 113–116, 1985.

[18] P. K. Stein and Y. Pu, "Heart rate variability, sleep and sleep disorders," *Sleep Med. Rev.*, vol. 16, pp. 47–66, 2012.

[19] C. Heneghan, P. D. Chazal, S. Ryan, C. P. Chua, L. Doherty, P. Boyle, P. Nolan, and W. T. McNicholas, "Electrocardiogram recording as a screening tool for sleep disordered breathing," *J. Clinical Sleep Med.*, vol. 4, no. 3, pp. 223–228, 2008.

[20] N. Marwan, N. Wessel, U. Meyerfeldt, A. Schirdewan, and J. Kurths, "Recurrence plot based measures of complexity and its application to heart rate variability data," *Phys. Rev. E*, vol. 66, no. 2, p. 026702, 2002.

[21] N. Marwan, M. C. Romano, M. Thiel, and J. Kurths, "Recurrence plots for the analysis of complex systems," *Phys. Rep.*, vol. 438, pp. 237–329, 2007.

[22] H. Poincare, "Sur la probleme des trois corps et les quations de la dynamique," *Acta Mathematica*, vol. 13, pp. 1–271, 1890.

[23] J. P. Eckmann, S. O. Kamphorst, and D. Ruelle, "Recurrence plots of dynamical systems," *Europhys. Lett.*, vol. 5, pp. 973–977, 1987.

[24] F. Takens, D. A. Rand, and L. S. Young, "Detecting strange attractors in turbulence," *Dynamical Syst. Turbulence*, vol. 898, pp. 366–381, 1981.
[25] M. Shelhamer, *Nonlinear Dynamics in Physiology: A State-Space Approach*. Hackensack, NJ, USA: World Scientific, 2007.
[26] A. C. Guyton and E. John, *Textbook of Medical Physiology*, 11th ed. Philadelphia, PA, USA: Elsevier, 2006.
[27] R. Klabunde, *Cardiovascular Physiology Concepts*. Riverwoods, IL, USA: Lippincott Williams & Wilkins, 2005.
[28] G. J. Tortora and N. P. Anagnostakos, *Principles of Anatomy and Physiology*, 6th ed. New York, NY, USA: Harper-Collins, 1990.
[29] A. Sagie, M. G. Larson, R. J. Goldberg, J. R. Bengston, and D. Levy, "An improved method for adjusting the QT interval for heart rate (the Framingham Heart Study)," *Amer. J. Cardiol.*, vol. 70, no. 7, pp. 797–801, 1992.
[30] G. L. Brengelmann, "A critical analysis of the view that right atrial pressure determines venous return," *J. Appl. Physiol.*, vol. 94, no. 3, pp. 849–859, 2003.
[31] H. Kantz and T. Schreiber, *Nonlinear Time Series Analysis*, 2nd ed. Cambridge, U.K.: Cambridge Univ. Press, 2004.
[32] M. Javorka, Z. Turianikova, I. Tonhajzerova, K. Javorka, and M. Baumert, "The effect of orthostasis on recurrence quantification analysis of heart rate and blood pressure dynamics," *Physiol. Meas.*, vol. 30, no. 1, pp. 29–41, 2009.
[33] C. L. Webber, Jr. and J. P. Zbilut, "Dynamical assessment of physiological systems and states using recurrence plot strategies," *J. Appl. Physiol.*, vol. 76, no. 2, pp. 965–973, 1994.
[34] J. B. Gao, "Recurrence time statistics for chaotic systems and their applications," *Phys. Rev. Lett.*, vol. 83, no. 16, pp. 3178–3181, 1999.
[35] G. Abandah and T. Malas, "Feature selection for recognizing handwritten Arabic letters," *Dirasat Eng. Sci. J.*, vol. 37, no. 2, pp. 242–256, 2010.
[36] P. Pudil, J. Novovicova, and J. Kittler, "Floating search methods in feature selection," *Pattern Recognit. Lett.*, vol. 15, pp. 1119–1125, 1994.
[37] R. Battiti, "Using mutual information for selecting features in supervised neural net learning," *IEEE Trans. Neural Netw.*, vol. 5, no. 4, pp. 537–550, Jul. 1994.
[38] N. Kwak and C. Choi, "Input feature selection by mutual information based on Parzen window," *IEEE Trans. Pattern Anal. Mach. Intell.*, vol. 24, no. 12, pp. 1667–1671, Dec. 2002.
[39] H. Peng, F. Long, and C. Ding, "Feature selection based on mutual information: Criteria of max-dependency, max-relevance, and min-redundancy," *IEEE Trans. Pattern Anal. Mach. Intell.*, vol. 27, no. 8, pp. 1226–1238, Aug. 2005.
[40] P. A. Estevez, M. Tesmer, C. A. Perez, and J. M. Zurada, "Normalized mutual information feature selection," *IEEE Trans. Neural Netw.*, vol. 20, no. 2, pp. 189–201, Feb. 2009.
[41] R. M. Fano, *Transmission of Information: A Statistical Theory of Communications*. New York, NY, USA: MIT Press, 1961.
[42] B. Guo and M. S. Nixon, "Gait feature subset selection by mutual information," *IEEE Trans. Syst., Man, Cybern. A: Syst. Humans*, vol. 39, no. 1, pp. 36–46, Jan. 2009.
[43] E. Parzen, "On the estimation of a probability density function and mode," *Ann. Math. Statist.*, vol. 2, no. 3, pp. 1065–1076, 1962.
[44] R. Gutierrez-Osuna, "Lecture notes on Introduction to Pattern Recognition," [Online]. Available: http://research.cs.tamu.edu/prism/lectures/pr/pr_l7.pdf
[45] S. Tulyakov, S. Jaeger, V. Govindaraju, and D. Doermann, "Review of classifier combination methods," *Stud. Computat. Intell.*, vol. 90, pp. 361–386, 2008.
[46] L. Xu, A. Krzyzak, and C. Y. Suen, "Methods for combining multiple classifiers and their applications to handwriting recognition," *IEEE Trans. Systems, Man, Cybern.*, vol. 23, no. 3, pp. 418–435, May/Jun. 1992.
[47] L. Lam and C. Y. Suen, "Application of majority voting to pattern recognition: An analysis of its behavior and performance," *IEEE Trans. Syst., Man, Cybern. A: Syst. Human*, vol. 27, no. 5, pp. 553–568, Sep. 1997.
[48] N. Littlestone and M. Warmuth, "Weighted Majority Algorithm," in *Proc. IEEE Symp. Found. Comput. Sci.*, 1989, pp. 256–261.
[49] B. Xie and H. Minn, "Real-time sleep apnea detection by classifier combination," *IEEE Trans. Inf. Technol. Biomed.*, vol. 16, no. 3, pp. 469–477, May 2012.
[50] J. Kittler, M. Hatef, R. Duin, and J. Matas, "On combining classifiers," *IEEE Trans. Pattern Anal. Mach. Intell.*, vol. 20, no. 3, pp. 226–239, Mar. 1998.
[51] C.-C. Chang and C.-J. Lin. (2011). LIBSVM—A library for support vector machines. *ACM Trans. Intell. Syst. Technol.* [Online]. *2(3)*, pp. 1–27. Software available at http://www.csie.ntu.edu.tw/∼cjlin/libsvm/
[52] Neural network toolbox, Mathworks. (2013). [Online]. Available: http://www.mathworks.com/products/neural-network/

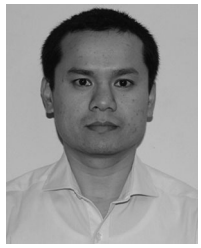

Hoa Dinh Nguyen received the B.S. and M.S. degrees in electrical engineering from Hanoi University of Science and Technology, Hanoi, Vietnam, and the Ph.D. degree in electrical engineering from Oklahoma State University, Stillwater, OK, USA, in 2000, 2002, and 2013, respectively.

From 2000 to 2004, he was an Engineer at Vietnam Television Technology Development and Investment Company. From 2004 to 2007, he was an Expert in Posts and Telecommunications Institute of Technology (PTIT), Hanoi, Vietnam. Currently, he is a Lecturer in information technology at PTIT. His research interests include feature selection, classification, decision fusion, statistical signal processing, database systems, and machine learning.

Brek A. Wilkins received the Ph.D. degree in biomedical sciences from Oklahoma State University Center for Health Sciences, Tulsa, OK, USA, in 2011.

He is currently a Postdoctoral Associate at Oklahoma State University Center for Health Sciences. He also serves as the Entrepreneurial Lead for an interdisciplinary group of biomedical and apparel engineers, where he oversees translational and commercialization processes associated with university technology. His professional research interests include biomedical signal analysis (nonlinear dynamics, vectorcardiography) and complex systems-based approaches to forecast cardiorespiratory disease and disorders.

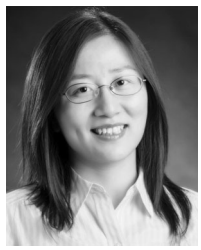

Qi Cheng (M'06–SM'12) received the B.E. degree in electrical engineering (highest honors) from Shanghai Jiao Tong University, Shanghai, China, in July 1999, and the M.S. and Ph.D. degrees in electrical engineering from Syracuse University, Syracuse, NY, USA, in 2003 and 2006, respectively.

From 1999 to 2000, she was a System Engineer at Guoxin Lucent Technologies Network Technologies Company, Ltd., Shanghai, China. Since August 2006, she has been with Oklahoma State University, Stillwater, OK, USA, where she is currently an Associate Professor with the School of Electrical and Computer Engineering. Her areas of interest mainly focuses on statistical signal processing and data fusion with applications in distributed sensor networks.

Dr. Cheng has served as an Associate Editor for the IEEE COMMUNICATIONS LETTERS. She is a Member of the Women in Engineering ProActive Network.

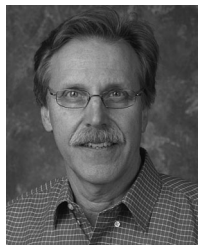

Bruce Allen Benjamin was born in Lincoln Nebraska, USA. He received the Ph.D. degree in cardiovascular physiology from the University of Oklahoma, Norman, OK, USA, in 1980.

From 1980 to 1984, he was a National Council Research Associate at NASA Ames Research Center at Moffett Field California. Since that time he held faculty positions at Texas A&M University College of Medicine and at Duke University Medical Center. Currently, he is the Associate Dean for Biomedical Sciences and Interim Vice Provost for Graduate Programs at Oklahoma State University Center for Health Sciences, Tulsa, OK. His professional activity lies in the field of cardiovascular dynamics.